Article:
Yu, J., Chang, W.-S., Zhang, R. et al. (2024) In-situ U-value measurements of typical building envelopes in a severe cold region of China: U-value variations and energy implications. Energy and Buildings, 324. 114947. ISSN: 0378-7788

https://doi.org/10.1016/j.enbuild.2024.114947

In-situ U-value Measurements of Typical Building Envelopes in a Severe Cold Region of China: U-value Variations and Energy Implications

Jiaqi Yu[a], Wen-Shao Chang[b], Ruinan Zhang[c,d], Yu Dong [c,d]*, Haoyu Huang[e], Tsung-Hsien Wang[a]

[a]*School of Architecture, University of Sheffield, Sheffield S10 2TN, United Kingdom;*

[b]*Lincoln School of Architecture and the Built Environment, University of Lincoln, Lincoln LN6 7TS, United Kingdom;*

[c] *School of Architecture and Design, Harbin Institute of Technology, Harbin, 150001, China*

[d] *Key Laboratory of Cold Region Urban and Rural Human Settlement Environment Science and Technology, Ministry of Industry and Information Technology, Harbin, 150001, China*

[e]*School of Engineering, Newcastle University, Newcastle NE1 7RU, United Kingdom*

* *Corresponding author*

ABSTRACT

Building energy consumption in the severe cold regions of China is an important consideration in building energy conservation because of the high amount of energy consumed by heating. As an important thermal parameter, the thermal transmittance (U-value) of building envelopes can directly affect the operational energy consumption of buildings. Understanding the U-values of buildings in severe cold regions is important to predict building energy accurately. However, the U-values of envelopes fluctuate constantly due to environmental impacts. Therefore, this study aimed to examine the influence of dynamic U-values on building energy efficiency. To achieve this, this study focused on the in-situ measurement of the U-values of two typical building envelopes in Harbin from winter to summer in 2023 to determine the average and dynamic U-values of the tested envelope, comprising a brick envelope and reinforced concrete (RC) envelope. The building energy simulation results based on theoretical U-values were compared with the measured average and dynamic U-values of the tested envelopes. The findings revealed that the fluctuations in the U-values were significant. In the dynamic U-values of tested brick and RC envelopes, the U-values in winter were 159.8% and 30.8% higher than those in summer, respectively. Furthermore, the dynamic U-values significantly influenced heating energy consumption, with an increase of up to 15.9%.

Keywords: In-situ U-value measurement; HFM method; Dynamic U-value; Residence energy consumption; Building envelopes

Nomenclature

RC	Reinforced concrete
HDD18	Heating design days (base temperature 18 ℃) [℃ · d]
CDD26	Cooling design days (base temperature 26 ℃) [℃ · d]
HFM	Heat flow meter
RHS-HFM	Removing the heat storage effect - heat flow meter
RH	Relative humidity [%]
U	Thermal transmittance [$W/(m^2 \cdot K)$]
R	Thermal resistance [$(m^2 \cdot K)/W$]
D	Thickness of the material [mm]
λ	Thermal conductivity of the material [$W/(m \cdot K)$]
q	Heat flow density [W/m^2]
T	Temperature [K]
ΔT	Temperature difference between indoor and outdoor environment [K]
G	Total solar energy transmittance
Subscripts	
mea	Measured
theo	Theoretical
se	External surface of the envelope
si	Internal surface of the envelope
out	Outdoor environment
in	Indoor environment
max	Maximum value
min	Minimum value
period, i	In the ith period
N	Total measurement duration
n	Number of periods comprising total duration of measurement

1 Introduction

The construction industry is an important contributor to energy consumption in all sectors across the world [1-3]. According to the International Energy Agency, the construction industry accounts for 36% of final energy use [4]. China's building energy use comprises one billion tons of standard coal, representing 21.7% of the country's total energy use [5]. In China, the building energy use in severe cold regions is enormous because of centralised heating systems with long-term heating periods [6]. For example, as a major city in a severe cold region, Harbin has 5 months per year when the centralised heating systems are activated [7]. The heating energy consumption in severe cold regions accounted for 24.1% of the total energy use of the construction industry in 2010 [8]. The building sector is regarded as one of the most cost-efficient fields for reducing energy consumption [9]. Consequently, numerous researchers have concentrated on developing building energy simulations to precisely manage energy usage and ensure a comfortable indoor environment for occupants [10-14].

As an important thermal parameter of the envelope, the U-value, also called thermal transmittance, directly affects building energy simulations, particularly cooling and heating energy use simulations [15-17]. Well-insulated envelopes have low U-values while poorly insulated envelopes have high U-values. In recent years, there has been notable growth in building energy simulation studies focusing on the effects of U-values on operational energy consumption [16, 18-21]. For example, Fernandes et al. used EnergyPlus to study the impact of U-value variations on building energy use in the Mediterranean region [20]. Their results revealed that an increase in the U-values can decrease the operational energy consumption in the lower northern latitudes. Building energy consumption was reduced by 20% when the U-value of envelopes increased from 0.15 to 0.3 $\mathrm{W/(m^2 \cdot K)}$ in Alexandria, Greece. Conversely, at higher northern latitudes, the operational energy consumption decreases with decreasing U-value. The operational energy consumption increased by 15% when the U-value of envelopes increased from 0.25 $\mathrm{W/(m^2 \cdot K)}$ to 0.5 $\mathrm{W/(m^2 \cdot K)}$ in Izmir. These studies indicate that different U-values significantly affect the operational energy simulation results. Therefore, the precise determination of U-values is essential for accurately predicting operational energy consumption.

In most existing building energy simulation studies, the U-value parameters are set to theoretical U-values rather than measured U-values [22-25]. The theoretical U-values of the envelopes can be calculated based on the thickness and thermal conductivity of every layer within building envelopes according to the ISO 6946 standard [26]. In an actual environment, several environmental factors can influence the thermal conductivity of building materials and the U-values of envelopes, most notably the atmospheric temperature and relative humidity (RH) [17, 24, 27, 28]. Thus, there is a discrepancy between the theoretical and actual U-values [25]. To obtain accurate U-values for envelopes in an actual environment, studies have conducted in-situ U-value measurements [29-32]. Four in-situ measurement methods have been used in past studies: heat flow meter (HFM), simple hot box-heat flow meter, thermometry, and quantitative infrared thermography method [17, 33-36]. Among these, the HFM method is a common method which necessitates the installation of a set of U-value measurement instruments in a tested room [37]. The standardised HFM method is governed by the ISO 9869-1 and ASTM C1155 standards [38, 39]. Numerous researchers have applied this method to measure the average U-values of building envelopes [29, 30, 32, 33, 40-46]. These results revealed a large discrepancy between the theoretical and measured average U-values of the building envelopes. For example, O'Hegarty investigated seven concrete walls with different structures using in-situ U-value measurements. The results showed that The measured U-values of the four tested walls were more than twice the theoretical U-values [27].

However, building energy simulations that involve inputting a single U-value cannot accurately reflect the real situation, even if the input U-value is the measured average U-value [25]. As environmental factors vary constantly, the hygrothermal behaviour of building materials is always changing, causing U-values to fluctuate [47]. The hygrothermal behaviour of building materials refers to the changes in their physical properties due to the absorbing, storing and releasing of heat, liquefying and vaporising of moisture [48]. This behaviour is associated with the microstructure of the building materials [49]. The microstructures of conventional building materials are inorganic and porous structures [50]. Changes in air temperature and RH affect the hygrothermal behaviour of building materials with different material porosities, including changes in the moisture content and internal temperature of materials [51]. Such changes affect the thermal conductivities of building materials [52, 53]. This results in dynamic U-values of the envelopes, as the U-value is positively correlated with the thermal conductivity of building materials [54]. Thus, compared to the theoretical and measured average U-values, the dynamic U-values were closer to the real conditions of the envelopes.

Several researchers have realised the existence and impact of dynamic U-values [55-57]. Dynamic U-values show that the thermal properties of building envelopes are unstable [24, 25]. However, few researchers have realised the impact of dynamic U-values on operational energy. Bruno and Bevilacqua applied WUFI software to simulate the dynamic U-values of three conventional walls in a Mediterranean climate [16]. The results revealed that the monthly variation in U-values was significant. The operational energy consumption results obtained from the dynamic U-values were higher than those obtained from the average U-values. This confirms that inputting dynamic U-values can significantly impact the operational energy simulation results. Notably, no studies have measured the dynamic U-values or used them for operational energy simulations.

Compared to a mild climate region, the energy conservation of building heating systems in a severe cold region is a noteworthy issue, as a cold region consumes more than three times as much heating energy as a temperate region [58, 59]. The dynamic U-values of envelopes in a severe cold region may significantly influence operational energy consumption. There are two existing research gaps in dynamic U-values and operational energy consumption in the severe cold region of China: (1) existing dynamic U-value data are not supported by actual measured data. Although many researchers have conducted in-situ U-value measurements, they have focused on average U-values rather than dynamic U-values [30, 44, 46, 60-62]. (2) Limited related studies focused on climate zone where buildings consume more energy, such as severe cold zone. Compared to mild climate zone, energy conservation of building heating system in severe cold zone is a noteworthy issue. Severe cold zone consumes more than three times as much heating energy as temperate zone [58, 59].

The novelty of this paper is studying the influences of measured dynamic U-values on simulation results of operational energy efficiency in severe cold regions of China. The study results expect to reduce the gap between building energy simulations and actual energy consumption by inputting the measured dynamic U-values. In-situ U-value measurements of typical brick and reinforced concrete (RC) envelopes were conducted from winter to summer in Harbin, China. The measurement method is according to the HFM method in ISO 9869-1 [38]. The measured average and dynamic U-values were obtained. The theoretical, average, and dynamic U-values were applied to the operational energy simulation. Finally, the operational energy results simulated by the three types of U-values were compared to quantitatively study the influence of the dynamic U-values of typical envelopes on the operational energy efficiency in a severe cold region of China.

2 Methods

The framework of this study is shown in Figure 1. The theoretical U-values of the tested envelopes were calculated based on the basic information of the tested envelopes and the average and dynamic U-values of the tested envelopes were obtained from the in-situ U-value measurements. Finally, the operational energy simulation results based on three types of U-values were compared.

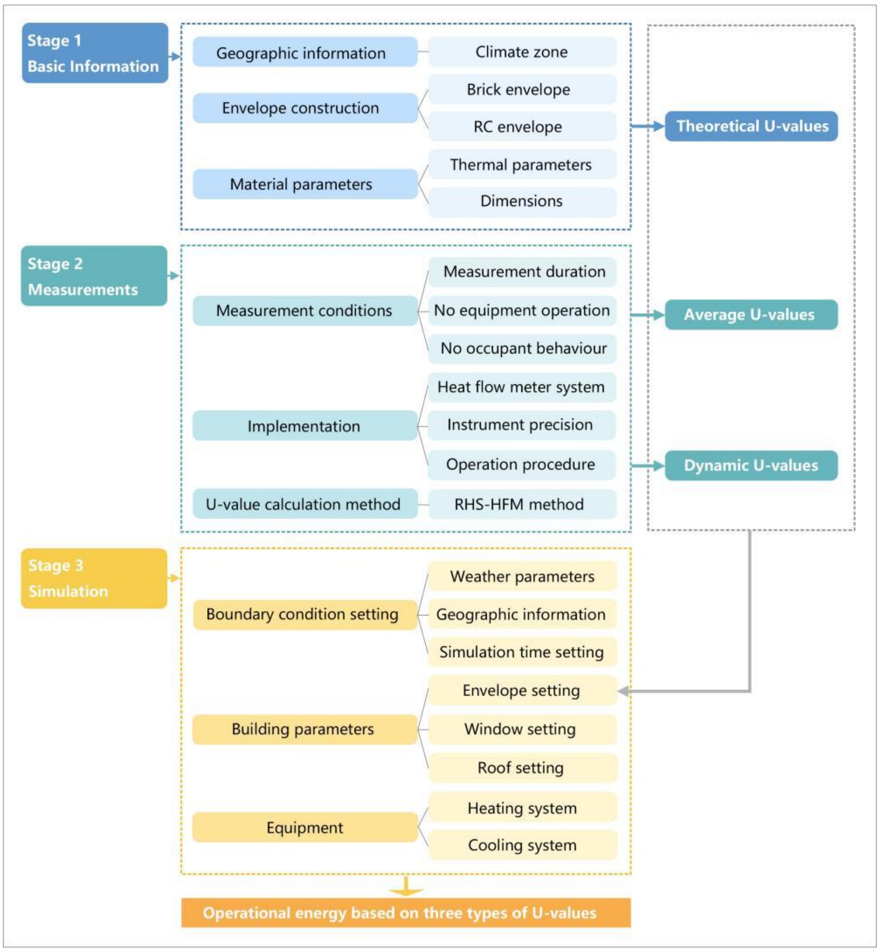

Fig. 1. Framework of the study

2.1. Weather Region of Harbin

Two typical external envelopes were tested in two residential buildings in Harbin, China. Harbin is located at latitude 45.7567°N and longitude 126.6424°E with a monsoon-influenced humid continental climate (Köppen climate classification: Dwa) [63]. Under the Code for Thermal Design of Civil Buildings in China (GB 50176-2016), China is divided into five main climate regions, and Harbin is situated in a severe cold region, as shown in Figure 2 [7]. Harbin is one of the major cities in the severe cold region of China, with a population of nearly 10 million [64]. The climate in Harbin varies greatly in different seasons. The difference between the average January and July temperatures in Harbin can be up to 40 ℃ [7]. This obvious temperature fluctuation is beneficial for observing and studying the fluctuation of U-values under different temperature conditions. In addition, Harbin has a large population, and it is significant to study building energy consumption in this region. Therefore, Harbin was chosen as the case city. Detailed meteorological information for Harbin is presented in Table 1.

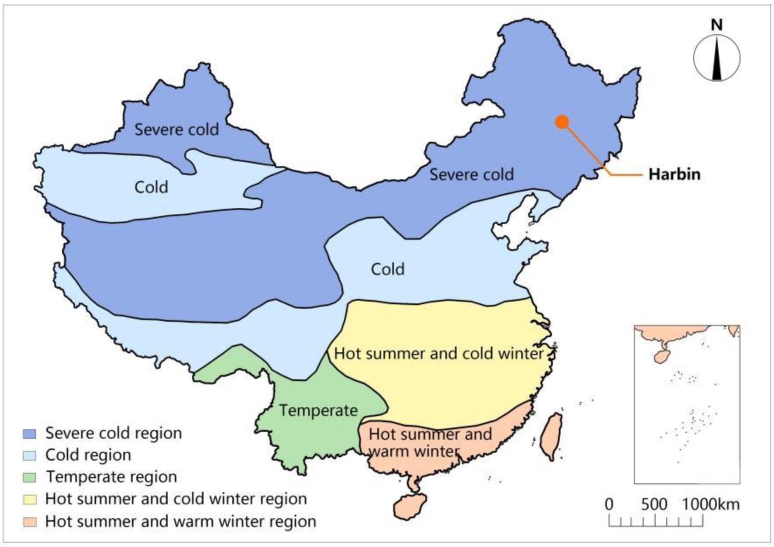

Fig. 2. Five climate regions of China.

Table 1. Meteorological information of Harbin

Parameter	Value
Climate region	Severe Cold Region
Average annual temperature	3.6 ℃
Average temperature of January	-16.9 ℃
Average temperature of July	23.8 ℃
Number of days with average daily temperatures below 5 ℃	167 days in a year
Heating design days (base temperature 18 ℃) (HDD18)	5032 ℃·d
Cooling design days (base temperature 26 ℃) (CDD26)	14 ℃·d

Data source: the Code for Thermal Design of Civil Building (GB 50176-2016) [7]

2.2. Tested envelopes

The two residential buildings tested were constructed in the 1980s and the 2010s using brick and RC constructions, respectively. The building envelopes of these two structures have been widely applied in the severe cold regions of Northeast China in recent decades. Before the 1990s, clay bricks were the principal building material in China. Clay is a non-renewable resource obtained from arable land that has caused the reduction and depletion of land resources; thus, the use of clay bricks was gradually restricted in the 2000s. Since the 2000s, concrete has replaced clay bricks as the primary building material in China [65].

Numerous brick buildings are built over three decades in Northeast China. The insulation performances of the envelopes are affected by material ageing in these buildings. According to existing studies, the measured U-values of envelopes of brick buildings around 30 years old were around twice the theoretical U-values of these envelopes, whereas the measured U-values of envelopes of brick buildings around 15 years old were around 1.3 times as much as the theoretical U-values of these envelopes [66]. It means that the actual insulation performance is lower than the expected insulation performance in older brick buildings.

Photographs of the test rooms and the room dimensions are shown in Figure 3. Both test rooms were bedrooms with one exterior envelope and one exterior window. The room and window dimensions of two test rooms were slightly different. This difference could have an effect on indoor temperature. According to the HFM method [38], the measured U-values were calculated by measuring the indoor and outdoor temperatures and heat flow density. Although dimensional factors affecting indoor temperature, they were not considered in the measured U-value calculation in this study. Case A was the brick envelope in test room A and Case B was the RC envelope in test room B. The test envelopes were multilayered. Detailed information on Cases A and B is presented in Table 2.

The theoretical U-values of the tested envelopes were obtained in accordance with ISO 6946 [26]. Using this method, the theoretical U-values can be estimated using the envelope parameters, as shown in Eqs.(1-2):

$$U = 1/(R_{se} + R_{si} + R_1 + R_2 + R_3 + \cdots + R_N)\ [W/(m^2 \cdot K)] \qquad (1)$$

$$R = D/\lambda\ [(m^2 \cdot K)/W] \qquad (2)$$

where R_{se} is thermal resistance of exterior surface, R_{si} is thermal resistance of interior surface, $R_1 + R_2 + R_3 + \cdots + R_N$ is the sum of thermal resistance of every layer within the envelope, D is the thickness of the building material, and λ is the thermal conductivity of the building material. In this study, R_{se} was estimated as 0.04 $(m^2 \cdot K)/W$ and R_{si} was estimated as 0.13 $(m^2 \cdot K)/W$ according to the ISO 6946 [26]. Based on the envelope parameters and Eqs.(1-2), the theoretical U-values for Cases A and B were calculated, as shown in Table 2.

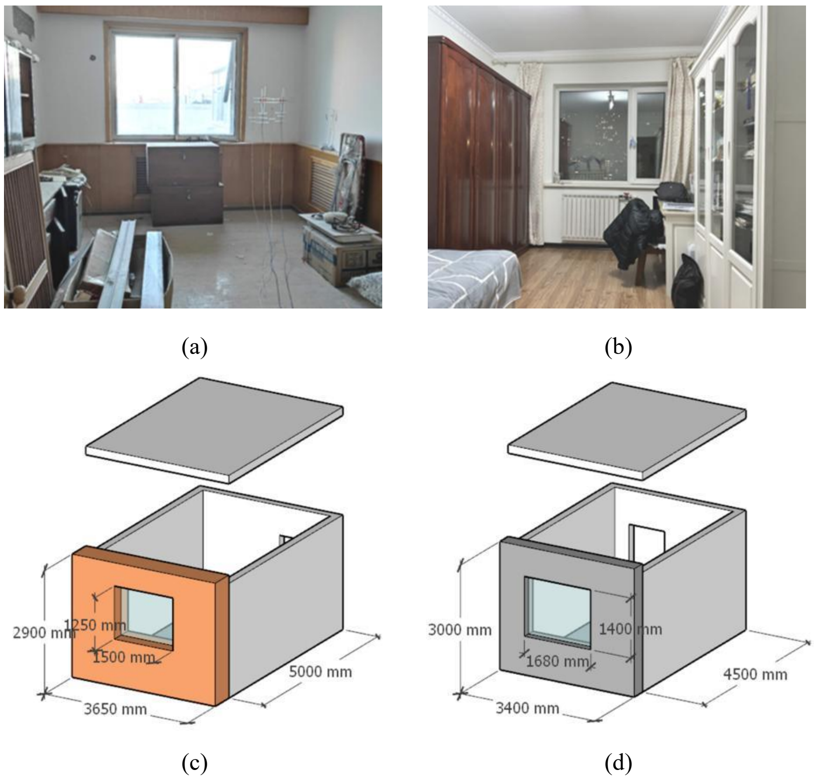

Fig. 3. In-site photos and room dimensions of the test rooms

(a) Photograph of test room A, (b) photograph of test room B, (c) model of test room A, and (d) model of test room B

Table 2. Building material dimensions and thermal properties of Cases A and B

Case		Material	Thickness [mm]	Conductivity [W/(m · K)]	Density [kg/(m³)]	Specific Heat Capacity [J/(kg · K)]	Layering sketch
A	1	Cement mortar	20	0.93	1800	1050	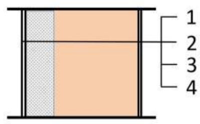
	2	EPS insulation	80	0.03	28.5	1650	
	3	Clay brick	240	0.78	1700	840	
	4	Cement mortar	10	0.93	1800	1050	
B	1	Cement mortar	15	0.93	1800	1050	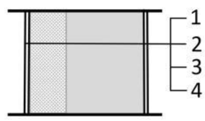
	2	EPS insulation	100	0.03	28.5	1650	
	3	Reinforced concrete	210	1.75	2500	920	
	4	Cement mortar	10	0.93	1800	1050	

Theoretical U-value: case A: 0.315 $W/(m^2 \cdot K)$; case B: 0.274 $W/(m^2 \cdot K)$

2.3. In-situ U-value measurements

2.3.1 Measurement conditions and instrumentation

Due to the huge temperature difference between the winter and summer in the severe cold region, the U-values of the building envelopes may fluctuate differently under different seasonal conditions. In order to comprehensively study the fluctuation of U-values in different seasons, the measurement period included summer, transition season, and winter. As shown in Table 3, the in-situ measurements were conducted from 17 January 2023 to 1 July 2023. Each tested envelope was measured six times, including three seasons, and each measurement lasted no less than twelve days to obtain reliable results according to ISO 9869-1 [38]. The measured dynamic U-values of each tested envelope included six values, which were the average U-values of the six measurement periods. To minimise the influence of human factors on the heat flow, no one entered the test rooms, and the windows and doors were kept closed during the measurement periods. There was no cooling system in the test rooms and the heating system was always switched off.

The in-situ U-value measurement system consisted of three parts: (1) two heat flux meters that generated an electrical signal when heat flowed through the tested envelopes; (2) indoor and outdoor environment recorders that recorded the temperature and RH every five minutes; and (3) a data logger for recording the measured heat flow every five minutes. A sketch of the tested envelope with all instruments is shown in Figure 4 (a), and the placement spots of heat flow sensors on the internal surfaces of two tested envelopes is shown in Figure 4(b) and 4(c). Photographs and parameters of the instruments are shown in Figure 5 and Table 4, respectively. Prior to the measurements, the tested envelopes were examined using an infrared imager to ensure homogeneous heat transfer in the tested area, as shown in Figure 5(b) and 5(d), respectively. All the instruments were calibrated by the manufacturer before use. The heat flux meters were installed at 1.5 m height from the floor to avoid incorrect measurements [67]. To reduce the influence of solar radiation on the U-value measurements, both tested envelopes were oriented north [38].

Table 3. In-situ U-value measurement periods of Cases A and B

Case No.	Measurement periods	Case No.	Measurement periods
Case A-1	2023.01.16–2023.01.29 (14D)	Case B-1	2023.02.02–2023.02.13 (12D)
Case A-2	2023.02.15–2023.03.01 (15D)	Case B-2	2023.03.03–2023.03.14 (12D)
Case A-3	2023.03.16–2023.03.31 (16D)	Case B-3	2023.04.03–2023.04.14 (12D)
Case A-4	2023.04.16–2023.04.29 (14D)	Case B-4	2023.05.01–2023.05.14 (14D)
Case A-5	2023.05.16–2023.05.31 (16D)	Case B-5	2023.06.02–2023.06.14 (13D)
Case A-6	2023.06.16–2023.07.01 (16D)	Case B-6	2023.07.03–2023.07.15 (13D)

Table 4. Parameters of instruments

Instrument	Brand	Model	Measuring range	Accuracy	Resolution
Heat flux meter	Hukseflux	HFP01	-2000 to +2000 W/m^2	± 3 %	0.001W/m^2
Indoor and outdoor	JDRK	COS-04	T: -40 to +80 ℃	T: ±0.1 ℃	T: 0.1 ℃
environment recorders			RH: 0 to +100%	RH: ±1.5%	RH: 0.1%
Data logger	Yustek	IUDAQ 256-8	NA	NA	NA

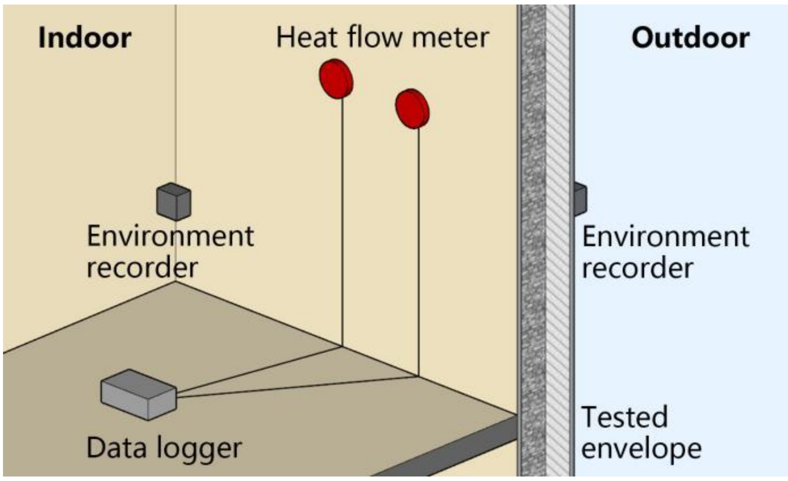

(a)

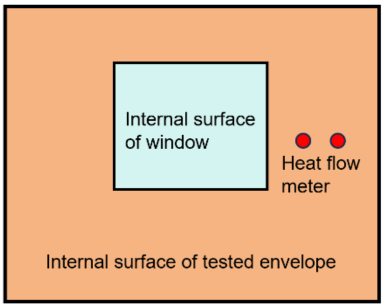

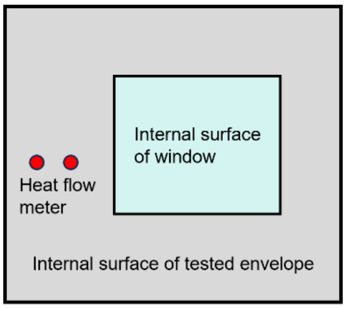

(b) (c)

Fig. 4. Sketches of tested envelopes

(a) The tested envelope with all instruments, (b) the placement of two heat flow sensors on the internal surface of the tested envelope in Case A, (c) the placement of two heat flow sensors on the internal surface of the tested envelope in Case B

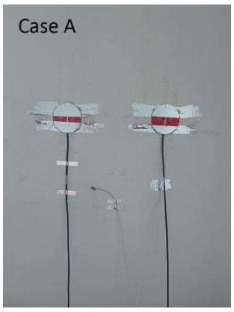

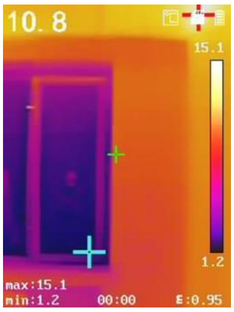

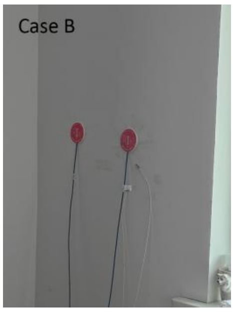

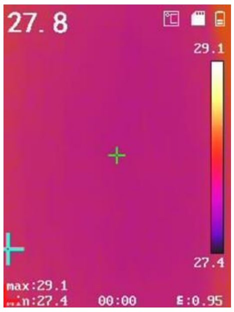

(a) (b) (c) (d)

(e) (f) (g)

Fig. 5. In-situ measurement photos

(a) Heat flux meters in Case A, (b) infrared image of Case A, (c) heat flux meters in Case B, (d) infrared image of Case B, (e) sensor of the outdoor environment recorder, (f) indoor environment recorder, and (g) set of data loggers

2.2.2 Removing the heat storage effect – heat flow meter (RHS-HFM) method

Because the measurement period included summer, the direction of the indoor and outdoor temperature differences sometimes changed. The changes in the direction of the heat flow were slower than the changes in the direction of the temperature difference owing to the heat storage capacity of the envelopes. This delay in the heat flow can lead to errors according to ISO 9869-1 [38]. To overcome errors caused by unstable temperature differences and heat flow, the removing the heat storage effect - heat flow meter (RHS-HFM) method was proposed by Shi et al. to remove the heat storage effect and overcome seasonal limitations [68] and has been the focus of many researchers [69-71]. According to this method, the average U-values and dynamic U-values consisting of the average U-values of the six measurement periods were calculated using Eqs.(3-6):

$$U = \frac{\overline{q_N}}{\overline{\Delta T_N}}\ [W/(m^2 \cdot K)] \tag{3}$$

$$\overline{\Delta T_N} = \frac{\sum_{i=1}^{n} \overline{\Delta T_{period,i}}}{n}\ [K] \tag{4}$$

$$\overline{\Delta T_{period,i}} \approx \frac{|T_{in,max} - T_{out,max}| + |T_{in,min} - T_{out,min}|}{2}\ [K] \tag{5}$$

$$\overline{q_N} = \frac{\sum_{i=1}^{n} \overline{|q_{period,i}|}}{n}\ [W/m^2] \tag{6}$$

The U-value equals the average temperature difference of total measurement duration ($\overline{\Delta T_N}$) divided by the average heat flow density of total measurement duration ($\overline{q_N}$), as formulated in Eq.(3). Compared with outdoor temperature fluctuations, indoor temperature fluctuations are delayed due to the heat storage effects of the envelopes. To remove the effects of heat storage, the calculation of $\overline{\Delta T_N}$ can be approximated and simplified, as shown in Eqs.(4-5). The total measurement duration (N) includes n periods of 24 hours each. $\overline{\Delta T_N}$ is the sum of average temperature difference of each period ($\overline{\Delta T_{period,i}}$) divided by the number of periods, as formulated in Eq.(4). In each period, $\overline{\Delta T_{period,i}}$ approximates the average of two values: (a) the temperature difference between the highest indoor temperature and the highest outdoor temperature and (b) the temperature difference between the lowest indoor temperature and the lowest outdoor temperature, as formulated in Eq.(5). $\overline{q_N}$ is the sum of the average heat flow densities for each period ($\overline{q_{period,i}}$) divided by the number of periods, as shown in Eq.(6).

2.3. Building energy simulation

The operational energy based on theoretical, average, and dynamic U-values was obtained through building energy simulations. EnergyPlus was used in this study because it has been widely adopted [69, 72, 73]. The building energy simulations were divided into two groups: Group A (the brick building) and Group B (the RC building). For each group, the reference building was simulated in Harbin by changing the U-values of the envelopes. For simulating building energy of each group based on the dynamic U-values, six simulations were performed to correspond to the six measurement periods. The input U-value was changed for each simulation. The input U-value in the simulation for each measurement period was the measured average U-value per period. Six simulations were also performed to estimate the building energy consumption based on the theoretical or average U-value. The input theoretical or average U-values were kept constant during each simulation.

Three types of U-values were applied to perform operational energy simulations for a reference building (Figure 6). The reference building is a widely used dwelling in a severe cold region of China. It consists of six floors, each with an area of 520 m^2. For each group, the simulation time was consistent with the measurement period. Weather files for Harbin were derived from in-situ measurements (T_{out} and RH_{out}) and weather station data during the measurement periods (solar radiation, wind speed, and direction). Because the two tested envelopes were built in different years in China, the major parameters of the building materials in Groups A and B were set according to two versions of the Design Standard for Energy Efficiency of Residential Buildings in Severe Cold and Cold Regions of China (JGJ 26-1986 and JGJ 26-2010) [74, 75], as shown in Table 5.

To investigate the effect of U-value changes on building energy consumption, all simulations were set to no occupants and no windows or doors were open. Heating and cooling systems only were activated when the indoor temperature was below 20 ℃ or above 27 ℃. To change the U-values of the envelopes without affecting the thermal mass of the envelopes, the envelopes of the reference building were set by changing the airgap thermal resistance to match the measured U-values in operational energy simulation [16]. Meanwhile, other parameters related to building materials were not changed.

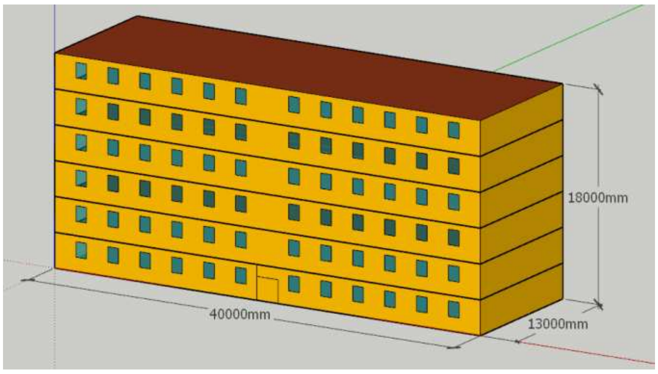

Fig. 6. Reference building model

Table 5. Major parameters of reference buildings in Group A and Group B

	Group A	Group B
Building envelope type	Brick envelope	RC envelope
Design standard	JGJ 26-1986	JGJ 26-2010
U-values of roof $[\mathrm{W}/(\mathrm{m}^2\cdot\mathrm{K})]$	0.2	0.2
U-values of floors $[\mathrm{W}/(\mathrm{m}^2\cdot\mathrm{K})]$	0.50	0.43
U-values of windows $[\mathrm{W}/(\mathrm{m}^2\cdot\mathrm{K})]$	1.85	1.55
G-value of windows	0.55	0.39
Infiltration ACH $[\mathrm{h}^{-1}]$	0.51	0.50

3 Results

3.1. Measured U-values of test envelopes

The indoor and outdoor temperatures and heat flow density in Cases A and B were recorded, and the measurement data are presented in Figures 7-8. During the measurement period (16/01/2023-15/07/2023), the outdoor temperature in Harbin varied significantly, with a minimum temperature of -28.7 ℃ in winter and a maximum temperature of 36.8 ℃ in summer. The indoor temperature in Case A varied from 16.0 ℃ to 32.4 ℃. The indoor temperature in Case B varied less, ranging from 19.7 ℃ 28.8 ℃. The indoor temperature in Cases A and B was approximately 20 °C in winter. Although the heating system was switched off in the test rooms, the neighbouring rooms contained heating systems that influenced the indoor environment. In Case A, the heat flow density was always positive in winter and early spring (Cases A-1 to A-4), indicating that the direction of the heat flow density did not change. In contrast, in late spring and summer (Cases A-5 and A-6), the heat flow density was sometimes negative, indicating a change in the direction of the heat flow. This is because the outdoor temperature is not always higher than the indoor temperature during late spring and summer in severe cold regions, and the direction of the temperature difference changed, resulting in a change in the direction of the heat flow. This phenomenon was also observed in Case B-6. Owing to the thermal storage of the envelopes, there was a delay in heat transfer, and the change in the direction of the temperature difference preceded the change in the direction of the heat flow density. If the heat transfer delay is not processed, the calculated U-value appears negative when the temperature difference is opposite the direction of the heat flow density, which leads to an error. Therefore, to reduce the effect of a delay in heat transfer, the RHS-HFM method was chosen to calculate the U-values of the envelopes.

As depicted in Figure 9, the measured U-values included dynamic and average U-values. The dynamic U-values in Case A included six values that were the average U-values for Cases A-1 to A-6. Meanwhile, the dynamic U-values in Case B included six values, which were the average U-values of Cases B-1 to B-6. The average U-value in each case was calculated based on the data for all the measurement periods. The average U-values exceed the theoretical U-values by 37.8% and 22.3% for Cases A and B, respectively. The dynamic U-values of Cases A and B displayed decreasing trends from winter to summer, which were more remarkable in Case A. For both Cases A and B, the U-values in winter exceeded those in summer by 159.8% and 30.8%, respectively. This indicates that the decrease in U-values from winter to summer was not negligible, especially for brick buildings built several decades ago.

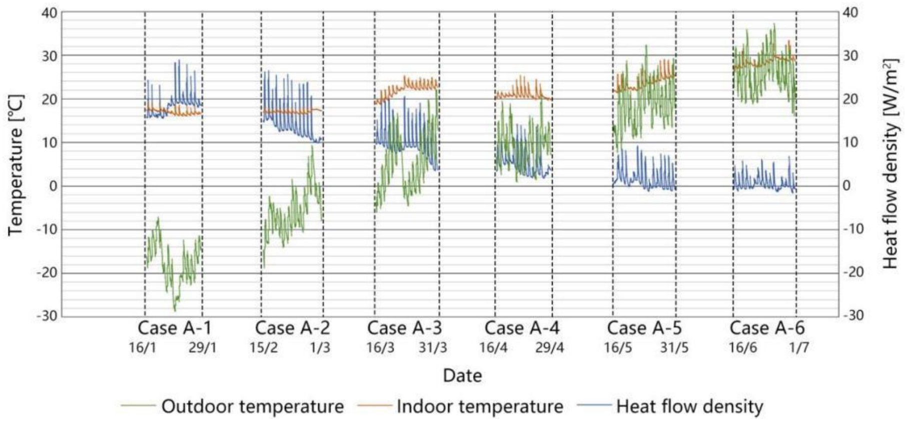

Fig. 7. Measured indoor and outdoor temperature and heat flow density in Case A

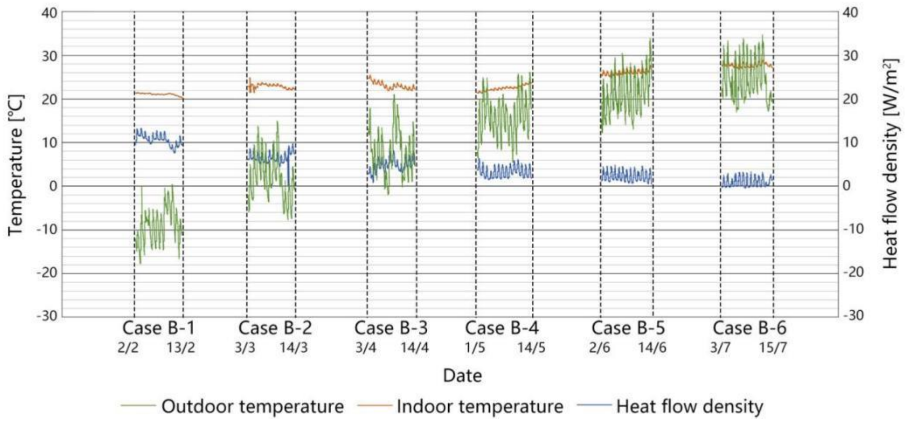

Fig. 8. Measured indoor and outdoor temperature and heat flow density in Case B

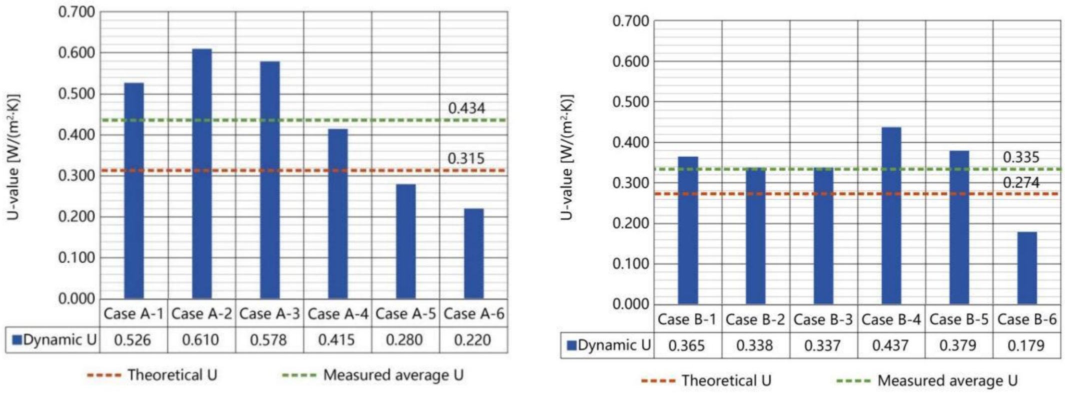

(a) (b)

Fig. 9. Theoretical and measured U-values in Cases A and B

(a) dynamic U-values for Case A; (b) dynamic U-values for Case B

3.2. Influence of dynamic U-values on operational energy efficiency in different buildings

The theoretical U-values, measured average U-values, and dynamic U-values of Cases A and B were applied to the building energy simulation of the reference building. The building energy simulations were divided into two groups: Groups A and B. Group A included six simulations, named Groups A-1 to A-6. The simulation times of the six simulations were based on the measurement periods in Case A (cases A-1 to A-6). Group B also included six simulations, named Groups B-1 to B-6; hence, the simulation times of the six simulations were based on the measurement periods in Case B (Cases B-1 to B-6). In all simulations, when the indoor temperature exceeded 20–27 ℃, the heating or cooling system was switched on.

The heating and cooling energy consumption based on the theoretical, average, and dynamic U-values in Groups A and B are presented in Figure 10. Figures 10 (a) and (b) show that the heating energy consumption is much more than the cooling energy consumption in Groups A and B. For example, heating energy consumption accounted for 98.2 % and 97.5 % of the total energy consumption in Groups A and B in the building energy consumption based on dynamic U-value, respectively. This result was related to the climatic region. In severe cold regions, heating energy is the major component of energy consumption, accounting for one-third of the total energy use [23].

As shown in Figure 10 (a), the heating energy consumption in Group A was 16.06 $\mathrm{kWh/m^2}$, 14.49 $\mathrm{kWh/m^2}$, and 13.18 $\mathrm{kWh/m^2}$ more than that in Group B according to building energy simulation results based on the dynamic, average, and theoretical U-values, respectively. It suggested that the more aged brick envelope had worse insulation properties compared to the RC envelope. Compared with the measured average U-values, the measured dynamic U-values exerted a more significant effect on heating energy. The influence of the measured dynamic U-values on heating energy consumption was more significant in Group A than in Group B. Figure 10 (a) shows that the heating energy based on the measured dynamic U-values exceeded that based on the theoretical U-values by 15.9% and 7.2% in Groups A and B, respectively. The heating energy based on the measured average U-values exceeded that based on the theoretical U-values by 8.1% and 5.4% for Groups A and B, respectively.

However, the differences of the cooling energy consumption between Groups A and B were not as significant as that of the heating energy consumption between Groups A and B. As shown in Figure 10 (b), the cooling energy consumption in Group A was more than 0.13 kWh/m^2, 0.17 kWh/m^2, and 0.15 kWh/m^2 more that in Group B according to building energy simulation results based on the dynamic, average, and theoretical U-values, respectively. In Groups A and B, the measured average and dynamic U-values showed insignificant differences in cooling energy consumption. The cooling energy based on the measured dynamic U-values was less than that based on the theoretical U-values by 2.1% in Group A. The cooling energy based on the measured dynamic U-values exceeded that based on the theoretical U-values by 3.0% in Group B. The cooling energy based on the measured average U-values exceeded that based on the theoretical U-values by 2.1% in Group A. The cooling energy based on the measured average U-values was less than that based on the theoretical U-values by 3.0 % in Group B.

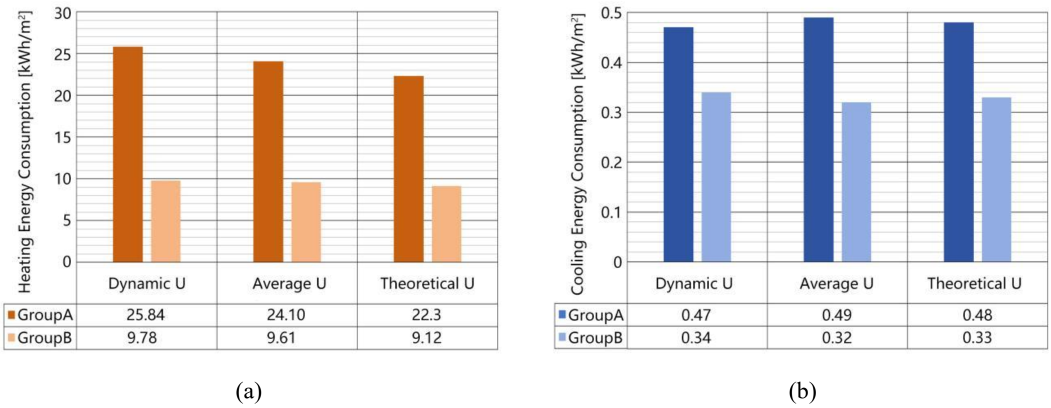

Fig.10. Operational energy simulation results for the reference building in both Group A and Group B based on different U-values

(a) Heating energy simulation results; (b) cooling energy simulation results

3.3. Influence of dynamic U-values on operational energy efficiency in different seasons

The heating and cooling energy consumption for each period is presented in Figure 11. The energy consumption based on the three types of U-values exhibited different characteristics during different seasons. The heating energy consumption in winter (including Groups A-1, A-2, and B-1) was higher than that in the transition season (including Groups A-3, A-4, A-5, B-2, B-3, and B-4). The gaps between the heating energy consumption based on the three types of U-values were more noticeable in winter than in the transition season. For example, in winter, the heating energy based on measured dynamic U-values exceeded that based on the theoretical U-values by 1.31 and 0.34 kWh/m^2 in Groups A-1 and B-1, respectively. The heating energy based on measured dynamic U-values exceeded that based on measured average U-values by 0.58 and 0.11 kWh/m^2 in Groups A-1 and B-1, respectively. In the transition season, the heating energy based on measured dynamic U-values exceeded that based on the theoretical U-values by 0.17 kWh/m^2 and 0.07 kWh/m^2 in Groups A-4 and B-4. The heating energy based on measured dynamic U-values was less than that based on measured average U-values by 0.03 kWh/m^2in Group A-4 and more than that based on measured average U-values 0.05 kWh/m^2 in Group B-4.

The gaps between the cooling energy consumptions based on the three types of U-values were unremarkable in summer (including Groups A-6, B-5, and B-6). The cooling energy based on measured dynamic U-values was less than that based on the theoretical U-values by 0.01 kWh/m^2 in Group A-6 and more than that based on the theoretical U-values by 0.01 kWh/m^2 in Group B-6. The cooling energy based on measured dynamic U-values was less than that based on measured average U-values by 0.02 kWh/m^2in Group A-6 and more than that based on measured average U-values 0.02 kWh/m^2 in Group B-6.

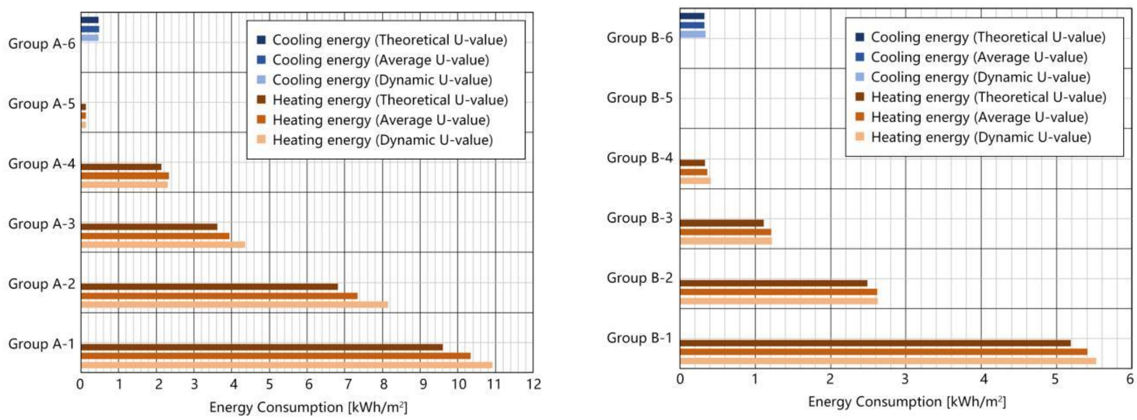

(a) (b)

Fig. 11. Detailed information on heating and cooling energy simulation results for both Group A (from A-1 to A-6) and Group B (from B-1 to B-6)

(a) Detailed simulation results for Group A and (b) detailed simulation results for Group B

4 Discussion

The decrease in U-values observed from winter to summer is a prominent phenomenon. During winter in severe cold regions, the porous materials containing moisture in the building envelopes are frozen and gradually thawed in the summer. According to existing studies, the thermal conductivity of pure ice is approximately 2.22 $W/(m \cdot K)$ at –10 °C, whereas that of water is 0.60 $W/(m \cdot K)$ at 20 ℃ [76]. The change in the physical state of the moisture within the envelopes from freezing to thawing may contribute to a decrease in the thermal conductivity of porous building materials. The U-values of the envelopes also decreased as they were proportional to the thermal conductivity of the building materials. Several researchers have reported similar findings for moisture-containing porous materials. For instance, Chuvilin et al. found that frozen porous sediments with high moisture contents had higher thermal conductivities than the unfrozen sediments [77]. Tang et al. revealed that the thermal conductivity of frozen soil-rock mixture decreased by 30.18% from -10 to 0 ℃ because of water-ice transition [78]. Vu et al. focused on the thermal conductivity of sandy soils in different states and revealed that the thermal conductivity of frozen sandy soils was considerably higher than that of unfrozen frozen sandy soils during the freeze–thaw process [79].

The decreasing trend in the U-values of the tested brick envelope was more significant than those of the tested RC buildings and the tested brick envelope had higher U-values in winter. The tested brick envelope has been built decades before the tested RC envelope, and it may have had a higher moisture content. There may be various reasons for the higher moisture content in the older brick envelope. For example, the deterioration of the building materials or technical weaknesses in the construction process may lead to an increased infiltration rate through the older brick envelope, thereby leading to a higher moisture content [66, 80, 81]. These findings illustrate the importance of moisture barriers in envelopes, especially old envelopes, to mitigate excessive heat loss during the heating-intensive season. Many buildings were built several decades ago in the severe cold regions of China. The insulation performance of these buildings does not meet contemporary building standard requirements [82, 83]. One of the practical retrofit options could be adding a moisture barrier to the external surface of envelopes to reduce heating energy use in winter.

Some cities in various countries have similar energy requirements with Harbin. The HDD18 and CDD26 of several typical cities are shown in Table 6, and data were derived from weather station data [84]. In-situ U-value measurements over the long term can contribute to improving heating energy consumption simulations in these cities. The inputs of both the measured dynamic and average U-values can influence the heating energy simulation. When simulating the long-term operational energy in a severe cold region, inputting the measured dynamic U-values could have a more significant impact on the heating energy simulation results of order brick buildings than those of newer RC buildings. However, the input of the measured U-values does not significantly affect the cooling energy simulation results. This may be associated with a relatively low proportion of cooling energy consumption in severe cold regions [85].

Table 6. The HDD18 and CDD26 of several typical cities

City	HDD18 [℃ · d]	CDD26 [℃ · d]
Harbin	5032	14
Oslo	4431	2
Helsinki	4312	8
Edinburgh	3138	1
Stockholm	3762	5
Reykjavík	4586	0

This study had three limitations: (1) only the northern envelopes were chosen for measurement to minimise the effects of solar radiation on the accuracy of the measurements. The dynamic U-values of the other oriented envelopes may have different characteristics, which require systematic and detailed research in the future. (2) In-situ measurements were conducted on only two envelopes for several months. In future studies, more envelopes with different orientations should be measured throughout the year to obtain more comprehensive data. The tested envelopes included not only conventional envelopes but also bio-based envelopes, such as cross-laminated timber envelopes. (3) The building parameters that affect U-values were not measured, such as infiltration rates of tested envelopes. In future studies, the infiltration rates of different envelopes can be measured, and the quantitative relationship between the dynamic U-values and the infiltration rates can be discussed. This relationship can explain the process that generates dynamic U-values more clearly. It can inform building maintenance, especially retrofitting of old buildings.

5 Conclusion

In-situ U-value measurements of two typical building envelopes in Harbin were conducted from winter to summer in 2023. The measured average and dynamic U-values of the brick and RC envelopes were obtained. To study the influence of dynamic U-values on building energy efficiency, the building energy simulation results based on the theoretical U-values, measured average U-values, and dynamic U-values of the tested brick and RC envelopes were compared. The main conclusions of this study are as follows.

(1) The fluctuations in U-values of typical building envelopes were substantial in severe cold regions. In the dynamic U-values of both brick and RC envelopes, the higher U-values were observed in winter months. The more aged brick envelopes displayed more significant U-value fluctuations than the RC envelopes. The higher U-values of typical building envelopes in winter may be attributed to the higher moisture content, illustrating the importance of moisture barriers in envelopes. In the severe cold regions of China, adding a moisture barrier should become an important retrofitting solution to reduce heating energy consumption in winter.

(2) The effect of dynamic U-values on the heating energy consumption of the reference brick building was greater than that of the reference RC building in severe cold regions. This indicates that inputting dynamic U-values can have a more significant impact on the heating energy simulation results of brick buildings built several decades ago than on those of newer RC buildings.

(3) The impact of dynamic U-values on operational energy consumption depends on the season in severe cold regions. The heating energy consumption based on dynamic U-values exceeded that based on theoretical U-values by 15.9% and 7.2% in the reference brick and RC buildings, respectively. Conversely, the differences between the cooling energy simulation results based on different types of U-values were not significant. This indicates that long-term dynamic U-value measurements could contribute to improving heating energy consumption simulations in severe cold regions.

This study contributes to minimising the gap between building energy simulations and actual energy consumption. Reliable measured data can be used to optimise building performance simulations and manage energy use more efficiently and accurately. This paper builds a foundation for further study on the dynamic U-values of different types of envelopes, including inorganic material envelopes and bio-based envelopes, in various climate regions. This dataset of dynamic U-values will provide more comprehensive and reliable references for building thermal attributes in building energy simulation.

Funding
This research is supported by Key Research and Development Program Project of Heilongjiang Province, China in 2023 (Innovation Base, JD2023SJ01).

Data availability
Data will be made available on request.

References

1. Reveshti, A.M., A. Ebrahimpour, and J. Razmara, *Investigating the effect of new and old weather data on the energy consumption of buildings affected by global warming in different climates.* International Journal of Thermofluids, 2023. **19**: p. 100377.
2. Cao, X., X. Dai, and J. Liu, *Building energy-consumption status worldwide and the state-of-the-art technologies for zero-energy buildings during the past decade.* Energy and Buildings, 2016. **128**: p. 198-213.
3. Guo, S., et al., *Global comparison of building energy use data within the context of climate change.* Energy and Buildings, 2020. **226**: p. 110362.
4. Li, H., et al., *Integrated building envelope performance evaluation method towards nearly zero energy buildings based on operation data.* Energy and Buildings, 2022. **268**: p. 112219.
5. Guo, Y.-Y., *Revisiting the building energy consumption in China: Insights from a large-scale national survey.* Energy for Sustainable Development, 2022. **68**: p. 76-93.
6. Chang, C., et al., *Data and analytics for heating energy consumption of residential buildings: The case of a severe cold climate region of China.* Energy and Buildings, 2018. **172**: p. 104-115.
7. Housing, M.o. and U.-R.D.o.t.P.s.R.o. China, *Code for Thermal Design of Civil Building (GB 50176-2016)*. 2016, China Architecture & Building Press Beijing, China.
8. Leng, H., et al., *Urban morphology and building heating energy consumption: Evidence from Harbin, a severe cold region city.* Energy and Buildings, 2020. **224**: p. 110143.
9. Nematchoua, M.K., et al., *Analysis of environmental impacts and costs of a residential building over its entire life cycle to achieve nearly zero energy and low emission objectives.* Journal of Cleaner Production, 2022. **373**: p. 133834.
10. Wang, P., et al., *Positivity and difference of influence of built environment around urban park on building energy consumption.* Sustainable Cities and Society, 2023. **89**: p. 104321.
11. Ni, S., et al., *Research on indoor thermal comfort and energy consumption of zero energy wooden structure buildings in severe cold zone.* Journal of Building Engineering, 2023. **67**: p. 105965.
12. Dougherty, T.R. and R.K. Jain, *Invisible walls: Exploration of microclimate effects on building energy consumption in New York City.* Sustainable Cities and Society, 2023. **90**: p. 104364.
13. Xu, H., et al., *LOD2 for energy simulation (LOD2ES) for CityGML: A novel level of details model for IFC-based building features extraction and energy simulation.* Journal of Building Engineering, 2023. **78**: p. 107715.
14. Choi, K., et al., *Review of infiltration and airflow models in building energy simulations for providing guidelines to building energy modelers.* Renewable and Sustainable Energy Reviews, 2023. **181**: p. 113327.
15. Klemp, S., A. Abida, and P. Richter, *A method and analysis of predicting building material U-value ranges through geometrical pattern clustering.* Journal of Building Engineering, 2021. **44**: p. 103243.
16. Bruno, R. and P. Bevilacqua, *Heat and mass transfer for the U-value assessment of opaque walls in the Mediterranean climate: Energy implications.* Energy, 2022. **261**: p. 124894.
17. Ficco, G., et al., *U-value in situ measurement for energy diagnosis of existing buildings.* Energy and Buildings, 2015. **104**: p. 108-121.

18. Ahern, C., B. Norton, and B. Enright, *The statistical relevance and effect of assuming pessimistic default overall thermal transmittance coefficients on dwelling energy performance certification quality in Ireland.* Energy and Buildings, 2016. **127**: p. 268-278.
19. Albatici, R., A.M. Tonelli, and M. Chiogna, *A comprehensive experimental approach for the validation of quantitative infrared thermography in the evaluation of building thermal transmittance.* Applied Energy, 2015. **141**: p. 218-228.
20. Fernandes, M.S., et al., *The impact of thermal transmittance variation on building design in the Mediterranean region.* Applied Energy, 2019. **239**: p. 581-597.
21. Ihara, T., A. Gustavsen, and B.P. Jelle, *Effect of facade components on energy efficiency in office buildings.* Applied Energy, 2015. **158**: p. 422-432.
22. Guo, H., et al., *A Comparison of the Energy Saving and Carbon Reduction Performance between Reinforced Concrete and Cross-Laminated Timber Structures in Residential Buildings in the Severe Cold Region of China.* Sustainability, 2017. **9**(8).
23. Dong, Y., et al. *Assessment of Energy Saving Potential by Replacing Conventional Materials by Cross Laminated Timber (CLT)—A Case Study of Office Buildings in China*. Applied Sciences, 2019. **9**, DOI: 10.3390/app9050858.
24. Kotsiris, G., et al., *Dynamic U-value estimation and energy simulation for green roofs.* Energy and Buildings, 2012. **45**: p. 240-249.
25. Yu, J., W.-S. Chang, and Y. Dong *Building Energy Prediction Models and Related Uncertainties: A Review*. Buildings, 2022. **12**, DOI: 10.3390/buildings12081284.
26. (ISO), I.O.f.S., *ISO 6946, Building components and building elements – Thermal resistance and thermal transmittance – Calculation method*. 2007.
27. O'Hegarty, R., et al., *In-situ U-value monitoring of highly insulated building envelopes: Review and experimental investigation.* Energy and Buildings, 2021. **252**: p. 111447.
28. Wang, Y., et al., *Experimental investigation on thermal conductivity of aerogel-incorporated concrete under various hygrothermal environment.* Energy, 2019. **188**: p. 115999.
29. Asdrubali, F., et al., *Evaluating in situ thermal transmittance of green buildings masonries—A case study.* Case Studies in Construction Materials, 2014. **1**: p. 53-59.
30. Gumbarević, S., et al. *Combining Deep Learning and the Heat Flux Method for In-Situ Thermal-Transmittance Measurement Improvement*. Energies, 2022. **15**, DOI: 10.3390/en15145029.
31. Evangelisti, L., et al., *A methodological approach for heat-flow meter data post-processing under different climatic conditions and wall orientations.* Energy and Buildings, 2020. **223**: p. 110216.
32. Gaspar, K., M. Casals, and M. Gangolells, *In situ measurement of façades with a low U-value: Avoiding deviations.* Energy and Buildings, 2018. **170**: p. 61-73.
33. Meng, X., et al., *Feasibility experiment on the simple hot box-heat flow meter method and the optimization based on simulation reproduction.* Applied Thermal Engineering, 2015. **83**: p. 48-56.
34. Bienvenido-Huertas, D., et al. *Determining the U-Value of Façades Using the Thermometric Method: Potentials and Limitations*. Energies, 2018. **11**, DOI: 10.3390/en11020360.
35. ISO, *ISO 9869-2,Thermal insulation — Building elements — In-situ measurement of thermal resistance and thermal transmittance — Part 2: Infrared method for frame structure dwelling*. 2018.

36. ASTM, *ASTM C1060,Standard Practice for Thermographic Inspection of Insulation Installations in Envelope Cavities of Frame Buildings.* 2011.

37. Ahmad, A., M. Maslehuddin, and L.M. Al-Hadhrami, *In situ measurement of thermal transmittance and thermal resistance of hollow reinforced precast concrete walls.* Energy and Buildings, 2014. **84**: p. 132-141.

38. ISO, *ISO 9869-1, Thermal Insulation, Building Elements, In-Situ Measurement of Thermal Resistance and Thermal Transmittance-Part 1: Heat Flow Meter Method*. 2014.

39. ASTM, *ASTM C1155-95 Standard, Standard Practice for Determining Thermal Resistance of Building Envelope Components from the In-situ Data*. 2007.

40. Mandilaras, I., et al., *Thermal performance of a building envelope incorporating ETICS with vacuum insulation panels and EPS.* Energy and Buildings, 2014. **85**: p. 654-665.

41. Evangelisti, L., et al. *In Situ Thermal Transmittance Measurements for Investigating Differences between Wall Models and Actual Building Performance*. Sustainability, 2015. **7**, 10388-10398 DOI: 10.3390/su70810388.

42. Gaspar, K., M. Casals, and M. Gangolells, *A comparison of standardized calculation methods for in situ measurements of façades U-value.* Energy and Buildings, 2016. **130**: p. 592-599.

43. Evangelisti, L., et al., *Experimental investigation of the influence of convective and radiative heat transfers on thermal transmittance measurements.* International Communications in Heat and Mass Transfer, 2016. **78**: p. 214-223.

44. Samardzioska, T. and R. Apostolska *Measurement of Heat-Flux of New Type Façade Walls*. Sustainability, 2016. **8**, DOI: 10.3390/su8101031.

45. Choi, D.S. and M.J. Ko *Comparison of Various Analysis Methods Based on Heat Flowmeters and Infrared Thermography Measurements for the Evaluation of the In Situ Thermal Transmittance of Opaque Exterior Walls*. Energies, 2017. **10**, DOI: 10.3390/en10071019.

46. Campbell, N., et al., *Monitoring the hygrothermal and ventilation performance of retrofitted clay brick solid wall houses with internal insulation: Two UK case studies.* Case Studies in Construction Materials, 2017. **7**: p. 163-179.

47. Lelievre, D., T. Colinart, and P. Glouannec, *Hygrothermal behavior of bio-based building materials including hysteresis effects: Experimental and numerical analyses.* Energy and Buildings, 2014. **84**: p. 617-627.

48. Wu, D., et al., *Dynamic hygrothermal behavior and energy performance analysis of a novel multilayer building envelope based on PCM and hemp concrete.* Construction and Building Materials, 2022. **341**: p. 127739.

49. Bennai, F., et al., *Assessment of hygrothermal performance of hemp concrete compared to conventional building materials at overall building scale.* Construction and Building Materials, 2022. **316**: p. 126007.

50. Islahuddin, M. and H. Janssen, *Hygric property estimation of porous building materials with multiscale pore structures.* Energy Procedia, 2017. **132**: p. 273-278.

51. Dong, W., et al., *A validation of dynamic hygrothermal model with coupled heat and moisture transfer in porous building materials and envelopes.* Journal of Building Engineering, 2020. **32**: p. 101484.

52. Wang, Y., et al., *Experimental study on the influence of temperature and humidity on the thermal conductivity of building insulation materials.* Energy and Built Environment, 2022.

53. Wang, Y., et al., *The impact of temperature and relative humidity dependent thermal conductivity of insulation materials on heat transfer through the building envelope.* Journal of Building Engineering, 2022. **46**: p. 103700.
54. Wang, Y., et al., *The effect of moisture transfer on the inner surface thermal performance and the thermal transmittance of the roof-wall corner building node in high-temperature and high-humidity areas.* Journal of Building Engineering, 2021. **44**: p. 102949.
55. Yang, X.e., et al., *Energy-saving potential prediction models for large-scale building: A state-of-the-art review.* Renewable and Sustainable Energy Reviews, 2022. **156**: p. 111992.
56. Franceschini, P.B. and L.O. Neves, *A critical review on occupant behaviour modelling for building performance simulation of naturally ventilated school buildings and potential changes due to the COVID-19 pandemic.* Energy and Buildings, 2022. **258**: p. 111831.
57. Chen, Y., et al., *Physical energy and data-driven models in building energy prediction: A review.* Energy Reports, 2022. **8**: p. 2656-2671.
58. Zou, Y., et al., *A simulation-based method to predict the life cycle energy performance of residential buildings in different climate zones of China.* Building and Environment, 2021. **193**: p. 107663.
59. Wan, K.K.W., et al., *Impact of climate change on building energy use in different climate zones and mitigation and adaptation implications.* Applied Energy, 2012. **97**: p. 274-282.
60. Krstić, H., et al. *Thermal Performance Assessment of a Wall Made of Lightweight Concrete Blocks with Recycled Brick and Ground Polystyrene*. Buildings, 2021. **11**, DOI: 10.3390/buildings11120584.
61. Ratnieks, J., A. Jakovics, and S. Gendelis, *Wall assemblies U-value calculation in test buildings using constant power heating.* Energy Procedia, 2018. **147**: p. 207-213.
62. Lucchi, E., *Thermal transmittance of historical brick masonries: A comparison among standard data, analytical calculation procedures, and in situ heat flow meter measurements.* Energy and Buildings, 2017. **134**: p. 171-184.
63. Peel, M.C., et al., *Updated world map of the Köppen-Geiger climate classification.* 2007. **11**(5): p. 1633-1644.
64. Statistics, H.B.o., *Seventh National Population Census*. 2020: https://www.harbin.gov.cn/haerbin/c104569/202105/c01_70396.shtml.
65. (NDRC), P.N.D.a.R.C., *Twelfth Five-Year Plan Guidance on Wall Materials Innovation* https://zfxxgk.ndrc.gov.cn/web/iteminfo.jsp?id=19709, 2011.
66. Byun, J., et al., *Proposal of a correction factor for predicting the thermal transmittance of building envelopes in existing buildings accounting for aging and environmental conditions.* Building and Environment, 2023. **243**: p. 110658.
67. Bienvenido-Huertas, D., et al., *Review of in situ methods for assessing the thermal transmittance of walls.* Renewable and Sustainable Energy Reviews, 2019. **102**: p. 356-371.
68. Shi, X., et al., *Investigation of a new kind of in-situ measurement method of thermal resistance of building envelope.* Energy and Buildings, 2022. **258**: p. 111803.
69. Bastos Porsani, G., et al., *Empirical evaluation of EnergyPlus infiltration model for a case study in a high-rise residential building.* Energy and Buildings, 2023. **296**: p. 113322.
70. Chen, L., et al., *A new method for measuring thermal resistance of building walls and analyses of influencing factors.* Construction and Building Materials, 2023. **385**: p. 131438.

71. Xing, L., et al., *A thermal balance method for measuring thermal conductivity by compensation of electric cooling or heating based on thermoelectric modules.* International Journal of Thermal Sciences, 2023. **189**: p. 108264.
72. Chen, Y., T. Hong, and M.A. Piette, *Automatic generation and simulation of urban building energy models based on city datasets for city-scale building retrofit analysis.* Applied Energy, 2017. **205**: p. 323-335.
73. Deshko, V., et al., *Evaluation of energy use for heating in residential building under the influence of air exchange modes.* Journal of Building Engineering, 2021. **42**: p. 103020.
74. *JGJ26-1986, Standard for energy conservation design of new heating residential buildings 民用建筑节能设计标准(采暖居住建筑部分).* 1986.
75. *JGJ26-2010, Design Standard for Energy Efficiency of Residential Buildings in Severe Cold and Cold Zones 严寒和寒冷地区居住建筑节能设计标准.* 2010.
76. Guo, S., et al., *Effective thermal conductivity of reservoir freshwater ice with attention to high temperature.* Annals of Glaciology, 2013. **54**(62): p. 189-195.
77. Evgeny, C., et al., *Effect of Ice and Hydrate Formation on Thermal Conductivity of Sediments*, in *Impact of Thermal Conductivity on Energy Technologies*, S. Aamir, Editor. 2018, IntechOpen: Rijeka. p. Ch. 7.
78. Tang, L., et al., *Thermal conductivity changing mechanism of frozen soil-rock mixture and a prediction model.* International Journal of Heat and Mass Transfer, 2023. **216**: p. 124529.
79. Vu, Q.H., J.-M. Pereira, and A.M. Tang, *Effect of clay content on the thermal conductivity of unfrozen and frozen sandy soils.* International Journal of Heat and Mass Transfer, 2023. **206**: p. 123923.
80. Yang, Y., et al., *In situ methodology for thermal performance evaluation of building wall: A review.* International Journal of Thermal Sciences, 2022. **181**: p. 107687.
81. d'Ambrosio Alfano, F.R., B.I. Palella, and G. Riccio, *Moisture in historical buildings from causes to the application of specific diagnostic methodologies.* Journal of Cultural Heritage, 2023. **61**: p. 150-159.
82. Liu, G., Y. Tan, and X. Li, *China's policies of building green retrofit: A state-of-the-art overview.* Building and Environment, 2020. **169**: p. 106554.
83. Wu, D., et al., *Uncertainty analysis of envelope retrofits for existing residential buildings in underdeveloped areas: A case study of Daokou, China.* Energy and Buildings, 2023. **284**: p. 112828.
84. Software, B., *Degree Days.net.* https://www.degreedays.net/, 2005.
85. Bo, R., et al., *Overheating of residential buildings in the severe cold and cold regions of China: The gap between building policy and performance.* Building and Environment, 2022. **225**: p. 109601.